Spin filter using a semiconductor quantum ring side-coupled to a quantum wire

Minchul Lee[1,2] and C. Bruder[1]

[1] *Department of Physics and Astronomy, University of Basel, CH-4056 Basel, Switzerland*
[2] *Department of Physics, Korea University, Seoul 136-701, Korea*

We introduce a new spin filter based on spin-resolved Fano resonances due to spin-split levels in a quantum ring (QR) side-coupled to a quantum wire (QW). Spin-orbit coupling inside the QR, together with external magnetic fields, induces spin splitting, and the Fano resonances due to the spin-split levels result in perfect or considerable suppression of the transport of either spin direction. Using the numerical renormalization group method, we find that the Coulomb interaction in the QR enhances the spin filter operation by widening the separation between dips in conductances for different spins and by allowing perfect blocking for one spin direction and perfect transmission for the other. The spin-filter effect persists as long as the temperature is less than the broadening of QR levels due to the QW-QR coupling. We discuss realistic conditions for the QR-based spin filter and its advantages to other similar devices.

PACS numbers: 85.75.-d, 71.70.Ej, 73.23.Hk, 05.10.Cc

Introduction.— Spintronics [1] that utilizes the electron's spin degree of freedom rather than its charge for information processing and storage has been a subject of intense interest in recent decades. The practical realization of spin-based electronic circuits requires the development of efficient means to generate spin-polarized currents, and to manipulate and detect spins. *Spin filters* that block the transport of one spin direction have been proposed as a device to generate and detect spin currents [2]. The basic scheme of a spin filter exploits spin-dependent transport through systems lacking time-reversal symmetry or having nontrivial geometric structures with spin-dependent interactions; such systems include ferromagnetic junctions [2], and nanostructures like quantum dots [3] (QD's) and rings [4, 5].

A simple but effective spin-filter implementation without coupling to magnetic materials has been suggested to exploit the *spin-dependent resonance* through a QD with Zeeman splitting that is embedded [3] in, or side-coupled [6, 7] to a quantum wire (QW). While in both cases the spin-dependent transport is based on scattering from spin-split QD levels and can be tuned by varying the gate voltage or the external magnetic field, the side-coupled configuration is more effective because the Fano resonance in this case can lead to *perfect blocking* of one spin direction and almost total transmission of the other. Side-coupled QD systems show two dips corresponding to the total suppression in the conductance of spin up and down [6, 7]. Since such spin filtering deteriorates rapidly with increasing temperature T, however, an ideal operation of the device requires large magnetic fields B or high g-factors such that $g\mu_B B \gg k_B T, k_B T_K$ where μ_B is the Bohr magneton and T_K is the Kondo temperature [7].

Recently, *quantum rings* (QR's) with Rashba spin-orbit coupling have been proposed for spin injection devices [5]. Spin precession due to the momentum-dependent effective magnetic field and the following spin interference of two quantum states propagating in opposite directions can not only modulate the charge conductance [8] but also induce spin currents through leads attached to the ring [5]. When an unpolarized charge current is injected through one of leads, quantum interference can produce pure spin currents through one of other leads. However, this interference-based spin-filter operation requires more than two leads to be linked to different positions of the QR.

In this Letter we propose another kind of spin filter that consists of a QR *side-coupled to* a QW; see Fig. 1(a). Spin-resolved Fano resonances due to spin-split levels formed in the QR in the presence of Rashba spin-orbit coupling and external magnetic fields [9] lead to a complete suppression of transport of either spin component at a set of gate voltage values, resulting in a series of valleys in the spin-resolved conductance. The separations between valleys are observed to be of the order of the Coulomb interaction energy. This QR-based spin filter has three advantages: (1) It does not require strong magnetic fields and high g-factors like the QD-based system. In the presence of spin-orbit coupling, a weak magnetic field applied to a small QR [10] can induce a large energy splitting between spin levels because it is the magnetic flux that causes the level splitting in the ring geometry. (2) Only a single contact of the QR to the external circuit such as leads or wires is necessary. (3) Finally, on-board tuning of polarization direction of spin currents is possible via the control of spin-orbit coupling strength.

Model.— First, we examine the energy level structure of a non-interacting QR with Rashba spin-orbit coupling in the presence of an external magnetic field. In the ideal one-dimensional limit where the radial width is much smaller than the radius R, only the lowest radial subband is occupied [11], and the effective Hamiltonian projected to the lowest radial mode can be written in polar

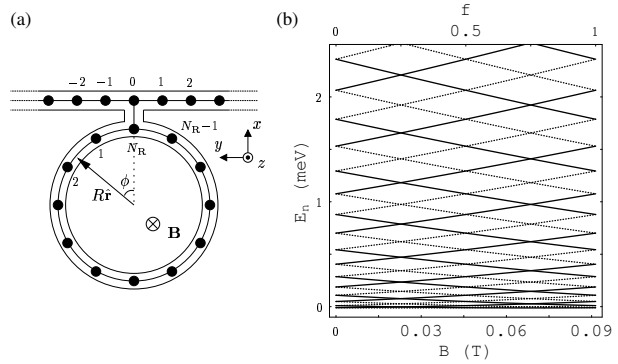

FIG. 1: (a) Schematic view of a quantum ring side-coupled to a quantum wire. Both systems are described by tight-binding models. The number of sites in the quantum ring is $N_{\rm R}$; in our study the limit $N_{\rm R}\to\infty$ is taken. (b) Energy spectrum of a non-interacting QR as a function of the magnetic field B or the corresponding flux f threading the QR with a radius $R = 120$nm. The dotted and solid lines correspond to spin index $\mu = +$ and $-$ levels, respectively. Here, the material parameters for GaAs are taken such that $m = 0.067m_e$ and $\alpha = 0.53\times10^{-11}$eVm in which case $2/|\cos\theta| = 3$.

coordinates [9]

$$\mathcal{H}_{\rm RN} = \frac{\hbar^2}{2mR^2}\left(i\frac{\partial}{\partial\phi}+f\right)^2 - \frac{\alpha}{2R}\{\boldsymbol{\sigma}\cdot\hat{\mathbf{r}}, i\frac{\partial}{\partial\phi}+f\}, \quad (1)$$

where m is the effective electron mass, $\boldsymbol{\sigma}$ the Pauli matrices, $\hat{\mathbf{r}}$ a unit vector in radial direction, and $\{A,B\} = AB+BA$. The energy of the radial mode is omitted. The spin-orbit coupling strength α defines the spin-flip length $l_{\rm so}\equiv\pi\hbar^2/m\alpha$, and the external magnetic field induces the normalized magnetic flux $f\equiv\pi BR^2/\Phi_0$ threading the ring; $\Phi_0 = hc/e$ is the flux quantum. The Zeeman splitting can be ignored compared to the kinetic energy $E_0\equiv\hbar^2/2mR^2$ as long as $1\gg g\mu_B B/E_0 = g(m/m_e)f$ is well satisfied; this holds in usual semiconducting materials with $f\lesssim 1$. Following the standard procedure [12], one can set up the tight-binding version of the Hamiltonian in terms of spin-μ electron operators $a_{n\mu}$, $a^\dagger_{n\mu}$ defined at site n of the QR, and the tight-binding Hamiltonian can be diagonalized through the Fourier transformation such that

$$\mathcal{H}_{\rm RN} = \sum_{m=1}^{N_{\rm R}}\sum_{\mu=\pm}\epsilon_{m\mu}d^\dagger_{m\mu}d_{m\mu}. \quad (2)$$

The operator $d^\dagger_{m\mu}$ creates an electron in orbital mode m and with spin index μ having space-dependent polarization $\hat{\mathbf{n}} = \hat{\mathbf{z}}\cos\theta+\hat{\mathbf{r}}\sin\theta$ that does not depend on the orbital index m due to the assumption that the Zeeman splitting is negligible [9]. In the limit $N_{\rm R}\to\infty$, the eigenenergy $\epsilon_{m\mu}$ is given by

$$\epsilon_{m\mu} = E_0\left[\left(m+f-\frac{1}{2}+\frac{\mu}{2\cos\theta}\right)^2+\frac{1}{4}\left(1-\frac{1}{\cos^2\theta}\right)\right] \quad (3)$$

with the polarization angle $\theta = \arctan[-N_{\rm so}]$, where $N_{\rm so}\equiv 2\pi R/l_{\rm so}$ is the number of spin flips around the ring. The resulting energy spectrum is periodic not only in f but also in $1/2\cos\theta$ (excluding the overall shift due to the last term in Eq. (3)). Moreover, the energy gaps between neighboring spin-split levels reach their maxima whenever $1/2|\cos\theta| = (2l+1)/4$, whereas the spin-splitting disappears at $1/2|\cos\theta| = l/2$, for integer $l>1$. Throughout our Letter $2/|\cos\theta|$ is assumed to be an odd integer to maximize the spin-splitting. Figure 1(b) shows the energy spectrum for realistic material parameters for GaAs. The ring size is taken to be $R = 120$nm, which is feasible using current fabrication technology [10]. The spectrum shows that a small magnetic field < 50mT is enough to induce a spin-splitting energy gap comparable to 1 to 3K. This large splitting that exists even in the absence of a strong external magnetic field definitely makes the QR a good candidate for ideal spin filter operation.

To take into account the electron-electron Coulomb interaction in the small QR, we adopt a simple capacitive model where the Coulomb interaction depends only on the total number of electrons: $\mathcal{H}_{\rm RI} = (U/2)\left[N^2-2N_gN\right]$ with $N\equiv\sum_{m\mu}d^\dagger_{m\mu}d_{m\mu}$. Here $U\equiv e^2/(C+C_g)$ and $N_{\rm g}\equiv C_gV/|e|$ denote the interaction strength and the gate charge (in units of $|e|$), respectively, in terms of self and gate capacitances, C and C_g.

The total Hamiltonian for a QR side-coupled to a QW can then be written as

$$\mathcal{H} = \mathcal{H}_{\rm RN}+\mathcal{H}_{\rm RI}+\mathcal{H}_{\rm W}+\mathcal{H}_{\rm WR} \quad (4)$$

with $\mathcal{H}_{\rm W} = -t_{\rm w}\sum_{n\mu}(c^\dagger_{n+1\mu}c_{n\mu}+h.c.)$ and $\mathcal{H}_{\rm WR} = t_{\rm wr}\sum_\mu(c^\dagger_{0\mu}a_{N_{\rm R}\mu}+h.c.)$, where the operator $c_{n\mu}$ ($c^\dagger_{n\mu}$) destroys (creates) an electron with spin index μ at site n of the wire. $\mathcal{H}_{\rm W}$ models the QW as an infinite tight-binding chain with a hopping energy $t_{\rm w}$ between neighboring sites, and $\mathcal{H}_{\rm WR}$ a spin-independent tunneling with strength $t_{\rm wr}$ between site 0 of the wire and site $N_{\rm R}$ of the ring. Note that the spin quantization axis for the QW has been rotated to align with the spin axis at site $N_{\rm R}$ of the QR, $\hat{\mathbf{n}}$ at $\hat{\mathbf{r}} = \hat{\mathbf{x}}$.

Spin filter.— We have calculated the zero-bias conductance G_μ for spin μ at the Fermi level $\epsilon_F = 0$ under the assumption that two electron reservoirs with nearly the same chemical potentials are attached at both ends of the QW [13]. The non-equilibrium scattering formalism [14] enables us to express the conductance in terms of the Green's function $\mathcal{G}^R_\mu(\epsilon)$ for a spin-μ electron at site 0 of the QW:

$$G_\mu = \frac{e^2}{h}\int d\epsilon\frac{\partial f(\epsilon)}{\partial\epsilon}\,{\rm Im}\,\Gamma(\epsilon)\mathcal{G}^R_\mu(\epsilon)\,. \quad (5)$$

Here, $f(\epsilon)$ is the Fermi distribution function with $\epsilon_F = 0$ and the symmetric coupling $\Gamma(\epsilon)$ of site 0 to the left and right sides of the QW is given by $\Gamma(\epsilon) = (2t_{\rm w}/\hbar)\sin\chi_{\rm w}(\epsilon)$ with $\chi_{\rm w}(\epsilon)\equiv\arccos[-\epsilon/2t_{\rm w}]$. In the non-interacting case

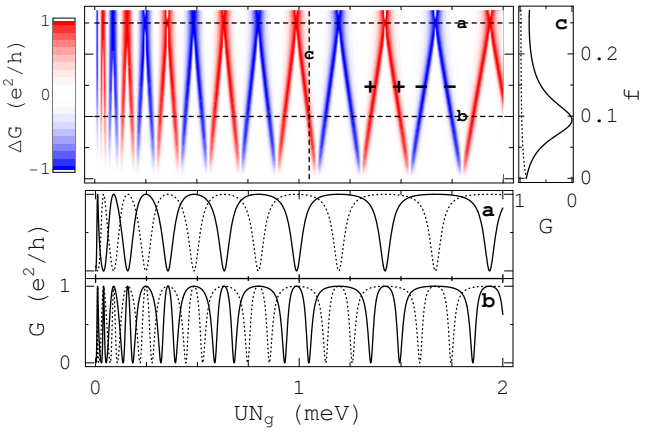

FIG. 2: (Color online) Net spin conductance ΔG as a function of gate voltage UN_g and magnetic flux f in the non-interacting case at zero temperature. The plus and minus signs indicate the sign of ΔG and are assumed to be repeated periodically along the UN_g axis. Here we have used the same QR parameter values as in Fig. 1(b) and set $t_{\rm w} = 5$meV, $t_{\rm wr} = 0.4$meV. The right and bottom figures show the spin-resolved conductances G_+ (dotted) and G_- (solid) taken along the dashed lines in the main figure.

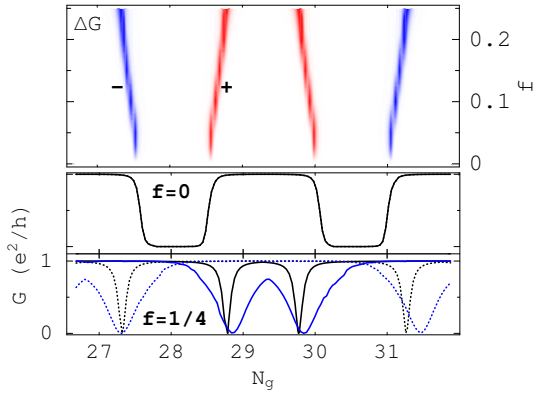

FIG. 3: (Color online) Net spin conductance ΔG as a function of gate charge N_g and magnetic flux f in the interacting case with $U = 0.5$meV. Lower figures show spin-resolved conductances $G_\pm$ for $f = 0$ and $1/4$, respectively. The same plot styles and parameter values as in Fig. 2 are used. For $f = 1/4$, the conductances (blue lines) with a larger coupling $t_{\rm wr} = 0.8$meV are also shown.

($C \ll C_g$ and $U \approx 0$), by solving the Dyson equation for $\mathcal{G}^R_\mu$, we obtain the spin-dependent transmission probability $T_\mu(\epsilon) = -\,\mathrm{Im}\,\Gamma(\epsilon)\mathcal{G}^R_\mu(\epsilon) = 1/(1+[Q_\mu(\epsilon)]^2)$ with $Q_\mu(\epsilon) \equiv \Gamma(\epsilon)^{-1}(t_{\rm wr}/\hbar)^2 \sum_m g^R_{m\mu}(\epsilon) = \Delta(\epsilon)\sum_m 1/(\epsilon - \epsilon_{m\mu})$, where $g^R_{m\mu}$ is the Green's function for the uncoupled QR and $\Delta(\epsilon) \equiv t^2_{\rm wr}/\hbar\Gamma(\epsilon)$ is the level broadening due to the QW-QR coupling. Since Q_μ diverges at $\epsilon = \epsilon_{m\mu}$, the transmission probability T_μ vanishes whenever a resonant state with spin μ is formed in the QR, giving rise to perfect suppression of the transport of spin-μ electrons. Note that this blocking condition is independent of any characteristics of the wire. Figure 2 shows the formation of a series of spin-split dips in the zero-bias conductances G_μ as functions of the gate voltage at zero temperature. The width of the valleys is restricted by the minimum of the energy splitting between neighboring levels and the level broadening $\Delta(\epsilon_F)$. The spin-dependent conductance can also be controlled by varying the flux f. The condition for total transmission ($T_\mu = 1$), $\sin 2\pi\sqrt{(\epsilon_F - UN_g)/E_0} = 0$, does not depend on spin, thus the peak positions in G_μ are the same for both spins.

This spin-dependent transmission generates a net spin flow through the wire: $\Delta G \equiv G_+ - G_- = (e^2/h)([Q_-]^2 - [Q_+]^2)/[(1+[Q_+]^2)(1+[Q_-]^2)]$ at zero temperature. The net spin conductance ΔG has local maxima or minima whenever one of the Q_μ diverges; see Fig. 2. The peak height in $|\Delta G|$ reaches almost the maximum value e^2/h if the spin splitting $\delta\epsilon$ is larger than the broadening $\Delta(\epsilon_F)$, in which case the unblocked states with opposite spin are transmitted almost completely. The ideal operation of the spin filter, therefore, requires $\delta\epsilon \gg \Delta(\epsilon_F)$. In addition, to avoid temperature-induced broadening through Eq. (5), both the spin splitting and the broadening should be larger than the temperature T as well. Interestingly, at $f = 1/4$, $|\Delta G|$ reaches e^2/h at its peaks regardless of UN_g, implying perfect blocking for one spin direction and perfect transmission for the other. Also, the peak widths are maximal at $f = 1/4$. This is related to the appearance of degenerate levels with the same spin at $f = 1/4$ [see Fig. 1(b)], which merges two peaks separated at $f \neq 1/4$ into one peak and strengthens the Fano resonances with broader width. This observation indicates that the best performance of the spin filter can be achieved at $f = 1/4$.

It should be noted that the polarization direction $\hat{\mathbf{n}} = \hat{\mathbf{z}}\cos\theta + \hat{\mathbf{x}}\sin\theta$ of the spin current can be rotated by tuning the strength of the spin-orbit coupling, which should be still adjusted to satisfy the odd-integer condition of $2/|\cos\theta|$ to achieve the maximal separation between spin-split levels. If the spin current is measured along a direction $\hat{\mathbf{n}}'$ other than $\hat{\mathbf{n}}$, the net spin current decreases via $\Delta G|_{\hat{\mathbf{n}}'} = \Delta G|_{\hat{\mathbf{n}}}\cos\zeta$, where ζ is the relative angle between $\hat{\mathbf{n}}$ and $\hat{\mathbf{n}}'$.

Coulomb interaction.— We now turn on the self-charging interaction in the QR with moderate values of U and investigate its effect on the transport at finite temperatures. The numerical renormalization group method, proven to be an excellent numerical tool for Anderson-type impurity systems, was applied to calculate the spin-resolved local density of states $\rho_\mu(\epsilon)$ on site N_R of the ring. The transmission amplitude can then be calculated using the Dyson equation: $T_\mu(\epsilon) = 1 - \pi\Delta(\epsilon)\rho_\mu(\epsilon)$.

Figure 3 shows the dependence of the zero-temperature conductances G_μ and ΔG on magnetic flux and gate voltage which has been tuned to such large values that high

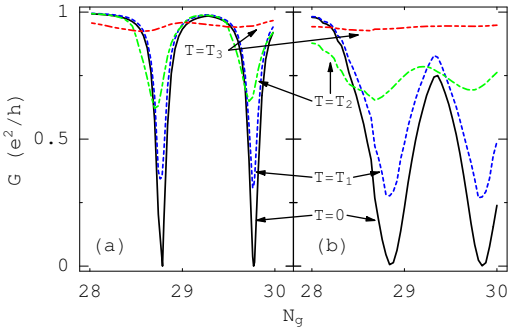

FIG. 4: (Color online) Finite-temperature conductance G_- for $f = 1/4$. The temperatures are given by $k_BT_1 = 0.13\Delta(\epsilon_F)$, $k_BT_2 = \Delta(\epsilon_F)$, and $k_BT_3 = 8.1\Delta(\epsilon_F)$. (a) $t_{\rm wr} = 0.4$meV and $\Delta(\epsilon_F) = 0.016$meV. (b) $t_{\rm wr} = 0.8$meV and $\Delta(\epsilon_F) = 0.064$meV. Other parameters as in Fig. 3.

QR levels with $\delta\epsilon \gg \Delta(\epsilon_F)$ contribute to the transport: the dips in conductance correspond to the QR levels with $m = 13$ and 14. At $f = 0$ the correlation between spin-degenerate QR levels and QW conduction electrons induces the Kondo effect whenever the QR contains an odd number of electrons. As a consequence, the Fano resonance due to the resultant effective resonant level at the Fermi level suppresses the charge transport regardless of the spin direction [15]. Each broad valley in G_μ at $f = 0$, however, splits into two spin-dependent sharp dips as the spin-splitting $\delta\epsilon$ due to finite magnetic field ($f \neq 0$) becomes larger than the Kondo temperature T_K. The Coulomb repulsion widens the separations between dips in G_μ or ΔG, which is now of the order of U [6, 7], or $\mathcal{O}(1)$ in terms of N_g even at $f = 1/4$, while the width of valleys, still of the order of $\Delta(\epsilon_F)$, is not affected. As long as $U > \Delta(\epsilon_F)$, the broadened separation due to the Coulomb interaction contributes toward perfect spin filtering at $f \neq 1/4$. As in the non-interacting case, the dip width increases as f goes to 1/4. For large QW-QR coupling, but still $\delta\epsilon > \Delta(\epsilon_F)$, the valleys can overlap, opening wide gate-voltage windows for inducing a finite spin current; see the uppermost figure in Fig. 3. Larger coupling with $\delta\epsilon \leq \Delta(\epsilon_F)$, however, leads to concurrent suppression of both spins and smaller net spin current.

Thermal fluctuations diminish the resonance-based suppression as soon as $k_BT \gtrsim \Delta(\epsilon_F)$; see Fig. 4. First, thermal broadening in the QW, via the smoothened peak in $\partial f/\partial\epsilon$, obscures the resonance as the temperature becomes comparable to the resonance width in $\rho_\mu(\epsilon)$, or the broadening $\Delta(\epsilon_F)$. Second, thermal fluctuations invoke transitions between QR levels that also weaken the resonance and consequently diminish the peak height in $\rho_\mu(\epsilon)$. The rapid degradation of the spin filter effect at $k_BT \approx \Delta(\epsilon_F)$ can be attributed to these thermal fluctuations. Consequently, our system will show ideal spin-filter operation if $k_BT \ll \Delta(\epsilon_F) \ll \delta\epsilon$. Since $k_BT_K \ll \delta\epsilon$ in most cases with $f \geq 0.1$, the Kondo temperature is irrelevant in spin filtering.

Discussion.— If the ring width is not narrow compared to the radius, higher radial modes will contribute to the transport. While the large energy gap between radial modes prohibits the direct excitation to higher modes at low temperatures, the spin can experience dephasing or relaxation due to the spin-orbit interaction that couples different radial modes with opposite spins [9]. Also, non-magnetic impurity scattering in such a thick ring with spin-orbit coupling can smear out the spin filtering.

Conclusions.— Our spin filter takes advantage of two ingredients: (1) the relatively large spin-splitting in a small QR with Rashba spin-orbit coupling and (2) the Fano resonances due to the spin-split levels in the QR that is side-coupled to a QW with one conduction channel. We predict perfect or considerable suppression of the transport of either of spin direction under real experimental conditions that are accessible using current technology.

We would like to thank V. Golovach and M.-S. Choi for helpful discussions. This work was financially supported by the SKORE-A program, the Swiss NSF, and the NCCR Nanoscience.

[1] G.A. Prinz, Science **282**, 1660 (1998); S.A. Wolf, D.D. Awschalom, R.A. Buhrman, J.M. Daughton, S. von Molnár, M.L. Roukes, A.Y. Chtchelkanova, and D.M. Treger, Science **294**, 1488 (2001).

[2] See, e.g., I. Zutić, J. Fabian, and S. Das Sarma, Rev. Mod. Phys. **76**, 323 (2004), and references therein.

[3] P. Recher, E.V. Sukhorukov, and D. Loss, Phys. Rev. Lett **85**, 1962 (2000); T.A. Costi, Phys. Rev. B **64**, 241310(R) (2001).

[4] D. Frustaglia, M. Hentschel, and K. Richter, Phys. Rev. Lett. **87**, 256602 (2001); M. Popp, D. Frustaglia, and K. Richter, Nanotechnology **14**, 347 (2003).

[5] A.A. Kiselev and K.W. Kim, J. Appl. Phys. **94**, 4001 (2003); S. Souma and B. Nikolić, Phys. Rev. Lett. **94**, 106602 (2005).

[6] M.E. Torio, K. Hallberg, S. Flach, A.E. Miroshnichenko, and M. Titov, Eur. Phys. J. B **37**, 399 (2004).

[7] A.A. Aligia and L.A. Salguero, Phys. Rev. B **70**, 075307 (2004).

[8] J. Nitta, F.E. Meijer, and H. Takayanagi, Appl. Phys. Lett. **75**, 695 (1999); D. Frustaglia and K. Richter, Phys. Rev. B **69**, 235310 (2004).

[9] F.E. Meijer, A.F. Morpurgo, and T.M. Klapwijk, Phys. Rev. B **66**, 033107 (2002); J. Splettstoesser, M. Governale, and U. Zülicke, Phys. Rev. B **68**, 165341 (2003).

[10] U.F. Keyser, C. Fühner, S. Borck, R.J. Haug, M. Bichler, G. Abstreiter, and W. Wegscheider, Phys. Rev. Lett. **90**, 196601 (2003); A. Fuhrer, T. Ihn, K. Ensslin, W.Wegscheider, and M. Bichler, Phys. Rev. Lett. **93**, 176803 (2004).

[11] A. Fuhrer, S. Lüscher, T. Ihn, T. Heinzel, K. Ensslin, W. Wegscheider, and M. Bichler, Nature (London) **413**, 822 (2001); U.F. Keyser, S. Borck, R.J. Haug, M. Bichler, G.

Abstreiter, and W. Wegscheider, Semicond. Sci. Technol. **17**, L22 (2002).
[12] S. Datta, *Electronic Transport in Mesoscopic Systems* (Cambridge University Press, Cambridge, 1995).
[13] O. Entin-Wohlman, C. Hartzstein, and Y. Imry, Phys. Rev. B **34**, 921 (1986).
[14] Y. Meir and N.S. Wingreen, Phys. Rev. Lett. **68**, 2512 (1992).
[15] K. Kang, Y. Cho, J.-J. Kim, and S.-C. Shin, Phys. Rev. B **63**, 113304 (2001).